NUMERICAL ANALYSIS AND MODELLING OF TOOL WEAR IN FRICTION STIR WELDING PROCESS

ERUKULA NARSIMHA[1] Dr.CHANDRA SEKHAR[2]

[1]M. Tech Student Department Of Mechanical Engineering, Malla Reddy College Of Engineering And Technology, Maisammaguda, Bahadurpally, Hyderabad, Telangana 500100

[2]Associate professor, Department Of Mechanical Engineering, Malla Reddy College Of Engineering And Technology, Maisammaguda, Bahadurpally, Hyderabad, Telangana 500100

Abstract *Friction Stir Welding (FSW) is a solid-state joining process that was invented in 1991; it is particularly useful for joints difficult to make using fusion techniques. Significant advances in FSW have been achieved in terms of process modelling since its inception. However, until now experimental work has remained the primary method of investigating tool wear in FSW. In this project, two main objectives were set; the first one was to produce a numerical approach that can be used as a useful tool to understand the effect that worn tool geometry has on the material flow and resultant weld quality. The second objective was to provide a modelling methodology for calculating tool wear in FSW based on a CFD model. Initially, in this study, a validated model of the FSW process was generated using the CFD software FLUENT, with this model then being used to assess in detail the differences in flow behaviour, mechanically affected zone (MAZ) size and strain rate distribution around the tool for both unworn and worn tool geometries. Later, a novel methodology for calculating tool wear in FSW is developed.*

Here a CFD model is used to predict the deformation of the highly viscous flow around the tool, with additional analysis linking this deformation to tool wear. A validation process was carried out in this study in order to obtain robust results when using this methodology. Once satisfied with the tool wear methodology results, a parametric study considering different tool designs, rotation speeds and traverse speeds was undertaken to predict the wear depth. In this study, three workpiece materials were used which were aluminium 6061, 7020 and AISI 304 stainless steel, swhile the materials used for the tools used were of H13 steel and tungsten-rhenium carbide (WRe-HfC) with different tool designs. The study shows that there are significant differences in the flow behaviour around and under the tool when the tool is worn and it shows that the proposed approach is able to predict tool wear associated with high viscous flow around the FSW tool. With a simple dome shaped tool, the results shows that the tool was worn radially and vertically and insignificant wear was predicted during welding near the pin tip.

However, in other regions the wear increased as the weld distance increased. Additionally, from the parametric study that was undertaken for the two tool designs - a dome and a conical shape- the study has found that for both tool designs, wear depth increases with increasing tool rotation speed and traverse speed. It was also shown that, generally, the wear depth was higher for the conical tool design than the dome tool in the pin tip zone. The research concludes that a proposed methodology is able to calculate tool wear associated with high viscous flow around the FSW tool, which could be used as a method for calculating tool wear without the need for experimental trials.

The CFD model has provided a good tool for prediction and assessment of the flow differences between un-worn and worn tools, which may be used to give an indication of the weld quality and of tool lifetime. Furthermore, from the results, it can be concluded that this approach is capable of predicting tool wear for different process parameters and tool designs and it is possible to obtain a low wear case by controlling the process parameters.

I. INTRODUCTION

Friction stir welding (FSW) is a solid-state joining process that has many advantages, including the ability to join high strength aluminium alloys, as well as dissimilar metals that are hard to join by conventional fusion techniques. The last two decades have seen significant advances in both tool material and tool design, allowing a wide range of materials to be welded (such as soft aluminium, magnesium alloys, hard carbon steels or stainless steel), with a range of thicknesses and desired weld quality in terms of a low number of defects and distortion. In addition, joint strengths that can reach those of the base material can be achieved. As the heat input in the process produces temperatures below the melting point, the advantages which are presented above are due to grain refinement in the weld nugget zone (WN) and in addition the lower temperature avoids solidification induced defects in the thermo-mechanically affected zone (MAZ). The FSW technique has many applications in the aeronautical, automotive and shipping industries and is considered to be energy efficient and environmentally friendly. Fundamentally, this process consists of three main parts, which are the tool, the work-piece(s) and the backing plate; the process is illustrated in Figure

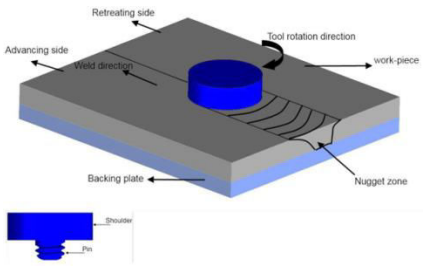

Fig 1: Friction stir welding process diagram

FSW is an extreme plastic deformation process where the flow regime is characterized by solid–state material flow. An analysis of the literature has shown that wear of the tool is very common during the FSW process and that this wear is associated with material flow during the process.

Although it has been shown that the FSW process has the ability to produce joints in various types of metals, tool integrity issues in terms of tool wear and tool life, seem to be one of the main restrictions for this technique at present, particularly when joining metal matrix composites (MMCs) and steel with a thickness of 6mm and above. While significant advances in FSW tool materials, such as the use of molybdenum-tungsten (Mo-W) alloys, polycrystalline cubic boron nitride (PCBN), cobalt (Co) based alloys and tungsten-rhenium (W–Re) alloys with the addition of hafnium carbide (HfC), have allowed the process to be used for increasingly demanding applications, the wear of FSW tools, which occurs in the form of tool degradation due to wear, has remained an issue. Recent developments in FSW have highlighted the fact that, until now, experimental work has remained the primary method of investigating tool wear in FSW.

II. LITERATURE REVIEWS

Schmidt et al. to calculate the heat generation in FSW. The analytical model included a slip-stick condition, which, it was argued, could make the model a more realistic representation of the FSW process. The stick condition will occur on the tool surface when the value of the frictional shear stress is higher than the material shear yield stress, in which case the velocity of the interface material has the same value as the velocity of tool surface. On the other hand, the slip condition occurs when the material slipping across the tool surface has a frictional shear stress value of less than that of the material shear yield stress.

Sadeghi et al. developed a coupled thermo-mechanical FE model of the FSW process implemented in the DEFORM and ABAQUS

codes in 2013. The output results of the DEFORM model was a thermal history in the workpiece, which was fed into the ABAQUS model, due to the fact that this methodology avoids excessive computational time. In this work, the DEFORM model was used to implement a rigid- viscoplastic material behaviour, while the ABAQUS model was used to implement elasto-plastic behaviour in order to obtain residual stress.

Zhang et al. examined the flow behaviour on the retreating side and advancing side in the FSW process. A 2D model was developed in order to understand the mechanism of FSW. The FEA model was created in the ABAQUS software and a slip –stick condition was implemented using equation 2-4, which was used as an upper limit for the value of shear stress. This was to provide less shear friction than shear yield, leading to a slip condition at the interface between the tool and welded material.

III. MODELLING METHODOLOGY

The concept of solving the fluid dynamics problem numerically using the Computational Fluid Dynamics (CFD) approach is also described. The nature of the problem solved in this work requires some extra capability on top of the standard CFD functions, in the form of material constitutive equations and user defined boundary conditions, these were formulated and implemented in the commercial software (ANSYS-Fluent) as User Defined Functions (UDF).

Structural hexahedral mesh study

In this study, a steady state 3D flow model of the FSW process was produced using the commercial CFD software FLUENT. This model was used to extract velocity values at particular positions in order to conduct a mesh independence study. It is solved isothermally, as used by Colegrove et al. [47] and Ji et al. [24] previously; this assumption was made as the flow stress of aluminium alloy 6061-T6 is relatively insensitive across the temperature range from 0.6 to 0.8Tm experienced in the welding process. The model assumptions, boundary conditions of the workpiece, solver and convergence criteria were defined based on the details included in the previous sections of this chapter. A stick condition [24, 47] has been applied on the tool surface to simplify the model for this case.

Mesh

The ICEM software was used to generate the structured HEXA-QUADRATIC mesh, and the aspect ratio of the cells around the tool was kept less than 7 for the all cells. The geometry was split into nine blocks and an O-Grid was used in the block of the tool (pin and shoulder) to get a good quality of mesh around the tool using biases. This type of mesh is flexible and was therefore used in this study to generate a very fine mesh with low cell distortion around the tool.

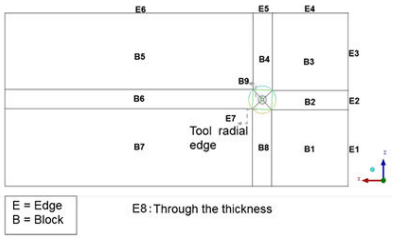

Fig 2: FSW model domain blocking strategy

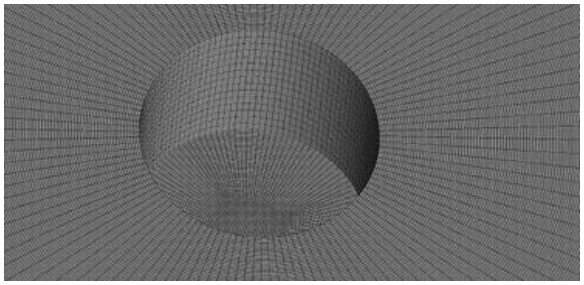

Fig 3: Hexahedral mesh shape at the tool surface

Material properties

The material used in the simulation was aluminium alloy 6061–T6, the material properties and the process parameters are presented in Table

Aluminium alloy 6061-T6 material properties

Material property	Value
Density, ρ	2700 Kg m^{-3}
A, material constant	8.863 $\times 10^{6}$ s^{-1}
α, material constant	0.045 $\times 10^{6}$ Pa $^{-1}$
n, material constant	3.55
Activation energy, Q_e	145 $\times 10^{3}$ J mol^{-1}
Gas constant, R	8.314 J K^{-1} mol^{-1}

Mesh study process parameters.

Weld parameter	Value
Inlet velocity, u_{weld}	3.39 mm s^{-1}
Tool Rotation speed, ω	770 rpm
Temperature (0.8 T_m)	684 K

Hybrid mesh study

In this study, the development of a hybrid mesh strategy was undertaken to determine appropriate tetrahedral cell size and developing the this mesh by including prism layers for the CFD modelling of the FSW process using complex tool geometry. To conduct a hybrid mesh study, the geometry, boundary conditions, material properties, solution control and methodology were the same as that used in the structured mesh study in section 4.6.1. The ICEM software was used to generate the hybrid mesh. Ideally, it is important to refine the mesh in the area of interest, which is mostly the plastic deformation area (zone around the tool) so that many cells are generated in that particular area.

IV RESULT AND DISCUSSION

Model 1 Results

The computational domain of model 1 was a rectangular cuboid 200 mm long, 100 mm wide and 0.4 mm thick. The diameter of the pin was 5 mm (a smooth cylinder) with a concave shoulder (2.5°) with a diameter of 13 mm.

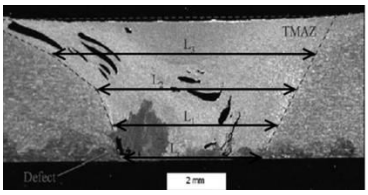

Fig 4: Weld zone measurement locations for validation data

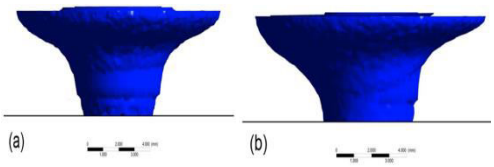

Fig 5: Predicated shape of the weld zone (a) case 1 at 1.66 mm s-1 and 300 rpm, (b) case 4 at 15 mm s-1 and 900 rpm

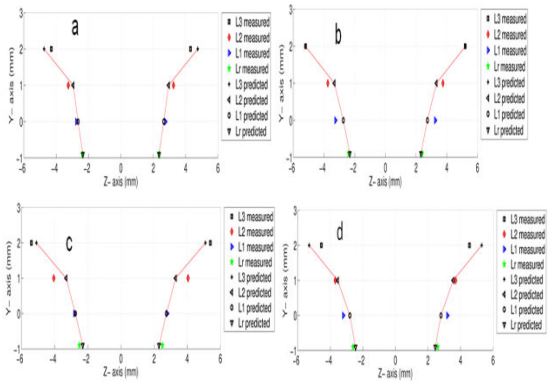

Fig 6: Measured and predicted values of the weld zone (in mm) (a) case 1 at 1.66 mm s-1 and 300 rpm, (b) case 2 at 1.66 mm s-1 and 600 rpm, (c) case 3 at 8.33 mm s-1 and 600 rpm and (d) case 4 at 15 mm s-1 and 900 rpm; using a viscosity of 1.5×106 Pa s

Computed temperature fields

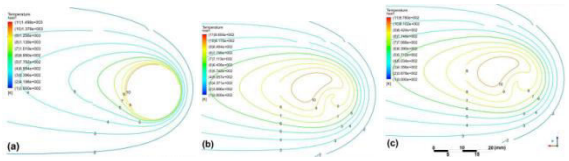

Fig 7: Plot of the temperature distribution at 2 ×10 3 mm weld distance: (a) on the top surface of the plate, (b) on a plane at the pin tip and (c) on the bottom surface of the plate for the initial geometry

Model 2 Results

Model 2 was used to conduct a mesh study using a threaded tool and used to compare the flow behaviour of the unworn and worn tools; the geometry of the computational domain of the model 2 was a rectangular cuboid with the dimensions presented in table. The unworn tool pin geometry for was a 1/4-20 UNC thread (6.35 major diameter with 12.7 mm pitch) constructed with PTC Creo software. The image of the worn tool was taken from the work of Prado et al. [10] and imported into PTC Creo and the tool geometry was constructed using this to approximately match the shape of the worn tool.

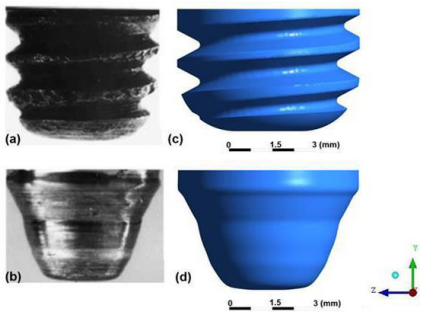

Fig 8: Geometry of the tools used for the study [10] (a) unworn and (b) worn and corresponding solid models used in the numerical simulation (c) unworn and (d) worn

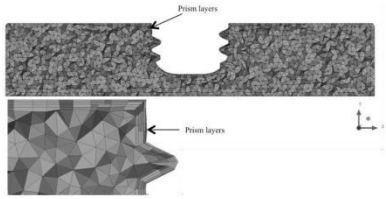

Fig 9: Mesh detail with prism layers at the tool surface

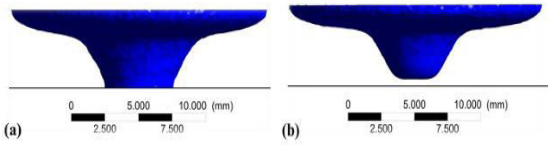

Fig 10: Shape of the weld zone at 1.66 mm s-1 and 300 rpm (a) unworn, (b) worn tool

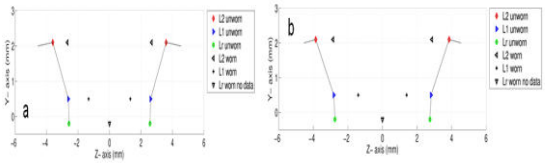

Fig 11: Predictions of the MAZ size [mm] for the unworn and worn tool geometries at 1.66 mm s-1;(a) 300 rpm and (b) 600 rpm

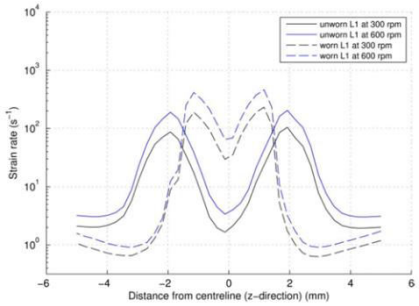

Fig 12: Strain rate distribution as a function of the distance from the axis of the tool rotation at Lr

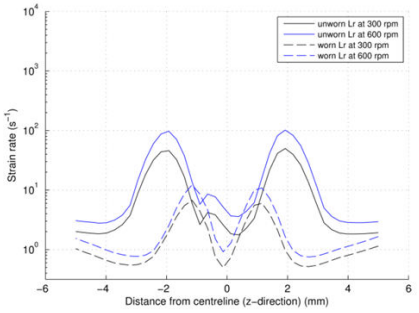

Fig 13: Strain rate distribution as a function of the distance from the axis of the tool rotation at Lr

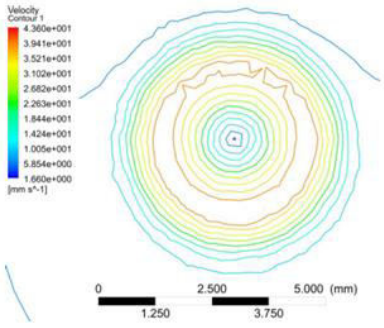

Fig 14: Velocity profile at 300 rpm for the unworn tool

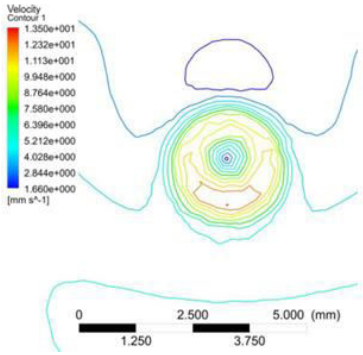

Fig 15: Velocity profile at 300 rpm for the worn tool

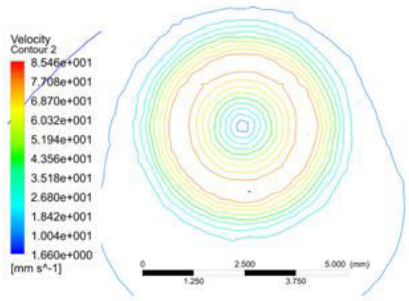

Fig 16: Velocity profile at 600 rpm for the unworn tool

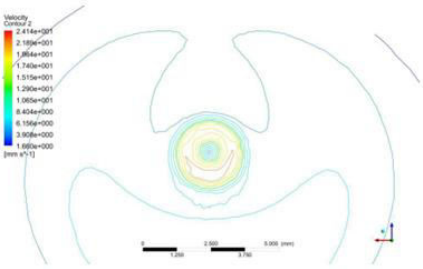

Fig 17: Velocity profile at 600 rpm for the worn tool

Computed temperature fields results

In this study, three x-z planes were used to plot the predicted temperature contours from the model at three positions through the thickness of the plate; the first plane was on the top surface of the plate, the second plane was at the pin tip, and the third plane was on the bottom surface of the plate. The simulated temperature contours are shown in Figure 6-6. It is evident that the peak temperature is on the top surface at the shoulder edge, and has a value of 1498K.

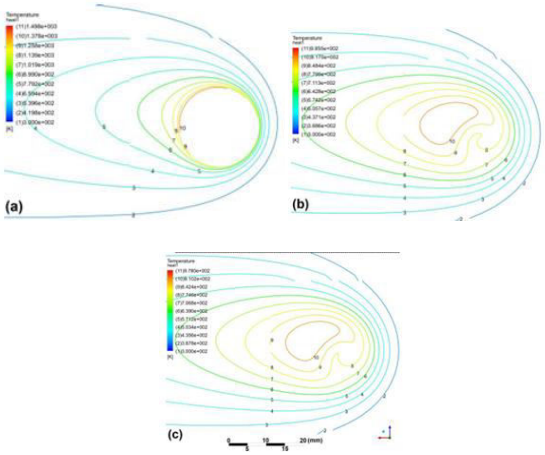

Fig 18: Plot of the temperature distribution at 2 ×10 3 mm weld distance: (a) on the top surface of the plate, (b) on a plane at the pin tip and (c) on the bottom surface of the plate for the initial geometry

Material flow behavior (velocity distribution and Pressure)

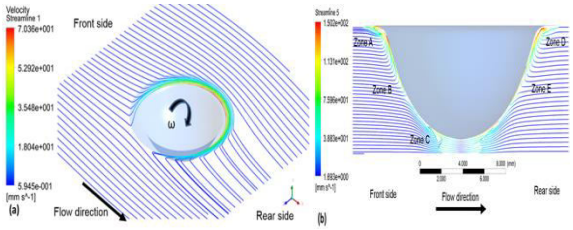

Fig 19: Stream-lines in different planes; (a) a horizontal x-z plane at the top surface of the plate, (b) x-y plane parallel to the flow direction for the initial geometry

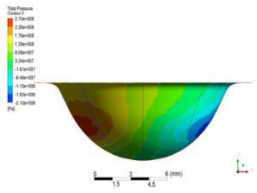

Fig 20: Pressure contours on the tool surface in the x-y plane parallel to the flow direction for the initial geometry

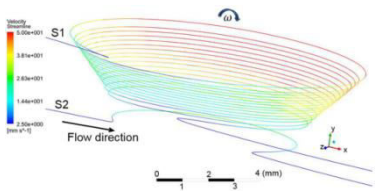

Fig 21: Stream-lines plots showing flow separation from the tool surface at 225 rpm and 2.5 mm s-1 weld speed. S1: stream line at mid pin zone; vertical position 3 mm, S2: stream line at tool tip zone; vertical position 0 mm

Tool wear prediction

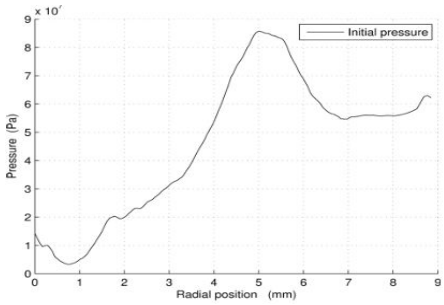

Fig 22: Average pressure distributions as a function of position on the tool for the initial geometry used for wear calculation

Wear depth results

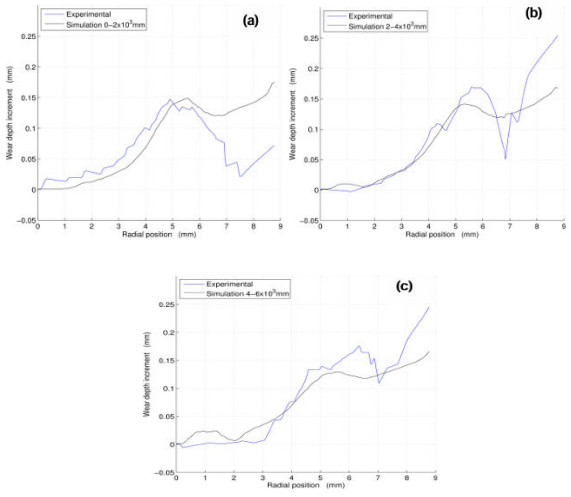

Fig 23: Plot of the wear depth along the tool surface after an increment of weld distances of; (a) 0-2×10 3 mm, (b) of 2- 4×10 3 mm, (c) of 4- 6×10 3 mm

Tool profile results

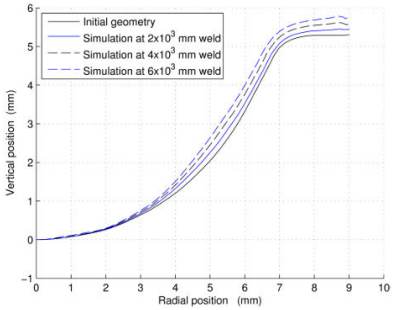

Fig 24: Tool profile after different welding distances

V CONCLUSIONS

A 3D-CFD model of the FSW process has been developed and used to compare the strain rate distribution and the size of the MAZ for the use of unworn and worn tool geometries at rotational speeds of 300 and 600 rpm. A validation process has been carried out in this study in order to obtain robust results when using the model. Unstructured grids with prism layers were also utilised to produce an optimise mesh quality for CFD modelling of the FSW process.

The key findings of the work can be summarised as follows:

1. A tetrahedral mesh takes a long time to solve; however, a hybrid mesh has been shown to be more computationally efficient in achieving an accurate solution for the FSW process and for modelling complex tool geometry.
2. Flow in the boundary layer is a crucial issue therefore a grid with a prism layer has been shown to be a powerful technique for solving this issue.
3. The results of the FLUENT CFD model showed a good agreement with an error of less than 15 % with the experimental data for the size of the MAZ. The predicted size and shape of the MAZ with the worn tool is shorter and about

2.5 mm smaller than that associated with the unworn tool.

4. The results of the strain rate and velocity distribution indicate a low stirring action for the worn tool, particularly near the weld root, potentially leading to defective weld joints.
5. The results of the shape of the weld zone showed the weld penetration does not reach to the bottom of the plate when tool becomes worn, which could affect the quality of the weld joint.

REFERENCES

[1]. P. Sinha, S. Muthukumaran, and S. Mukherjee, Analysis of first mode of metal transfer in friction stir welded plates by image processing technique. Journal of Materials Processing Technology, 2008. 197(1): p. 17-21.

[2]. M. Sued, D. Pons, J. Lavroff, and E. Wong, Design features for bobbin friction stir welding tools: Development of a conceptual model linking the underlying physics to the production process. Materials & Design, 2014. 54: p. 632-643.

[3]. R. S. Mishra and Z. Ma, Friction stir welding and processing. Materials Science and Engineering: R: Reports, 2005. 50(1): p. 1-78.

[4]. N. McPherson, A. Galloway, S. Cater, and M. Osman. A comparison between single sided and double sided friction stir welded 8mm thick DH36 steel plate. in Trends in Welding Research 2012: Proceedings of the 9th International Conference. , 2013.

[5]. ASM International. D. Lohwasser and Z. Chen, Friction stir welding: From basics to applications, 2009: Elsevier.

[6]. A. Toumpis, A. Galloway, L. Molter, and H. Polezhayeva, Systematic investigation of the fatigue performance of a friction stir welded low alloy steel. Materials & Design, 2015. 80: p. 116-128.

[7]. Y. J. Chao, X. Qi, and W. Tang, Heat transfer in friction stir welding—experimental and numerical studies. Journal of manufacturing science and engineering, 2003. 125(1): p. 138-145.

[8]. M. Selvaraj, A temperature dependent slip factor based thermal model for friction stir welding of stainless steel. Sadhana, 2013. 38(6): p. 1393-1405.

[9]. W. Thomas, P. Threadgill, and E. Nicholas, Feasibility of friction stir welding steel. Science and Technology of Welding & Joining, 1999. 4(6): p. 365-372.

[10]. R. Prado, L. Murr, K. Soto, and J. McClure, Self-optimization in tool wear for friction-stir welding of Al 6061+ 20% Al2 O3 MMC. Materials Science and Engineering: A, 2003. 349(1): p. 156-165.

[11]. D. Choi, C. Lee, B. Ahn, J. Choi, Y. Yeon, K. Song, H. Park, Y. Kim, C. Yoo, and S. Jung, Frictional wear evaluation of WC–Co alloy tool in friction stir spot welding of low carbon steel plates. International Journal of Refractory Metals and Hard Materials, 2009. 27(6): p. 931-936.

[12]. H. Bhadeshia and T. DebRoy, Critical assessment: friction stir welding of steels. Science and Technology of Welding & Joining, 2009. 14(3): p. 193-196.

[13]. P. A. Colegrove and H. R. Shercliff, 3-Dimensional CFD modelling of flow round a threaded friction stir welding tool profile. Journal of Materials Processing Technology, 2005. 169(2): p. 320-327.